AD-A191 441 TRANSMITTING BOUNDARY FOR FINITE-DIFFERENCE CALCULATIONS WITH FINITE MODE.. (U) SCIENCE APPLICATIONS INTERNATIONAL CORP SAN FRANCISCO CA W YEUNG ET AL. 1/1

UNCLASSIFIED 20 NOV 87 AFOSR-TR-87-1754 AFOSR-85-0023 F/G 20/1 NL

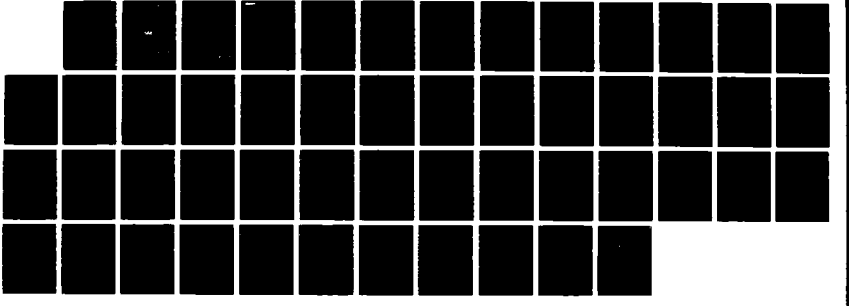

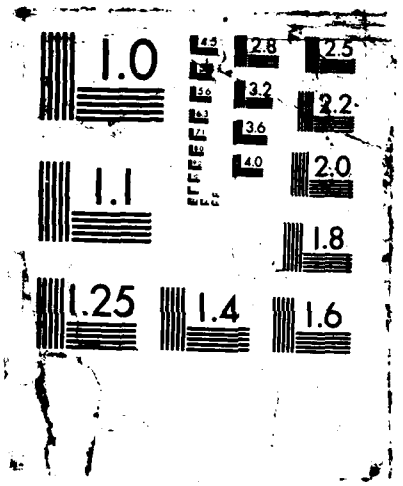
1.0
1.1
1.25
1.4
1.6
1.8
2.0
2.2
2.5
2.8
3.2
3.6
4.0

AFOSR-TR- 87-1754

TRANSMITTING BOUNDARY FOR FINITE-DIFFERENCE CALCULATIONS WITH FINITE MODELING OF AN INFINITE MEDIUM

SAIC™
Science Applications International Corporation

TRANSMITTING BOUNDARY FOR FINITE-DIFFERENCE CALCULATIONS WITH FINITE MODELING OF AN INFINITE MEDIUM

November 20, 1987

Submitted to:

U.S. Department of the Air Force
AFOSR/PKZ
Bolling Air Force Base
Washington, D.C. 20332-6448

Submitted by:

Mr. William Yeung
and
Dr. Michael B. Gross

Science Applications International Corporation
160 Spear Street, Suite 1250
San Francisco, California 94105

REPORT DOCUMENTATION PAGE

1a. REPORT SECURITY CLASSIFICATION	1b. RESTRICTIVE MARKINGS
2a. SECURITY CLASSIFICATION AUTHORITY	3. DISTRIBUTION / AVAILABILITY OF REPORT Approved for public release; distribution unlimited.
2b. DECLASSIFICATION / DOWNGRADING SCHEDULE	
4. PERFORMING ORGANIZATION REPORT NUMBER(S)	5. MONITORING ORGANIZATION REPORT NUMBER(S) AFOSR-TR- 87-1754
6a. NAME OF PERFORMING ORGANIZATION: Science Applications International Corp. / 6b. OFFICE SYMBOL (If applicable)	7a. NAME OF MONITORING ORGANIZATION: AFOSR/NM
6c. ADDRESS (City, State, and ZIP Code): 160 Spear St. Suite 1250 San Francisco, CA 94105	7b. ADDRESS (City, State, and ZIP Code): AFOSR/NM Bldg 410 Bolling AFB DC 20332-6448
8a. NAME OF FUNDING / SPONSORING ORGANIZATION: AFOSR / 8b. OFFICE SYMBOL (If applicable): NM	9. PROCUREMENT INSTRUMENT IDENTIFICATION NUMBER: AFOSR-85-0023
8c. ADDRESS (City, State, and ZIP Code): AFOSR/NM Bldg 410 Bolling AFB DC 20332-6448	10. SOURCE OF FUNDING NUMBERS

PROGRAM ELEMENT NO.	PROJECT NO.	TASK NO.	WORK UNIT ACCESSION NO.
61102F	2304	A3	

11. TITLE (Include Security Classification)

Transmitting Boundary for Finite-Difference Calculations With Finite Modeling of an Infinite Medium

12. PERSONAL AUTHOR(S)
Mr. William Yeung & Dr. Michael B. Gross

13a. TYPE OF REPORT	13b. TIME COVERED	14. DATE OF REPORT (Year, Month, Day)	15. PAGE COUNT
Final	FROM 1 Dec 84 TO 30 Apr 86	Nov. 20, 1987	47

16. SUPPLEMENTARY NOTATION

17. COSATI CODES			18. SUBJECT TERMS (Continue on reverse if necessary and identify by block number)
FIELD	GROUP	SUB-GROUP	

19. ABSTRACT (Continue on reverse if necessary and identify by block number)

The purpose of this effort was to study the construction of novel energy absorbing boundary conditions for use at the artificial far field boundaries of exterior wave problems. One approach was pursued which involves the superposition of the solutions for a fixed boundary and for a free boundary. An analytic model was used to identify the cause of the small errors that result in the cancellation process of this approach. This model showed that the appropriate velocity at the free boundary has to be modified when the computational time step is less thatn the maximum stable time step. First and second order corrections have been developed.

20. DISTRIBUTION / AVAILABILITY OF ABSTRACT	21. ABSTRACT SECURITY CLASSIFICATION
☐ UNCLASSIFIED/UNLIMITED ☐ SAME AS RPT ☐ DTIC USERS	

22a. NAME OF RESPONSIBLE INDIVIDUAL	22b. TELEPHONE (Include Area Code)	22c. OFFICE SYMBOL
Maj John Thomas	(202) 767-5026	NM

DD FORM 1473, 84 MAR — 83 APR edition may be used until exhausted. All other editions are obsolete.

1.0 INTRODUCTION

One of the common problems in numerical simulations of nonlinear response in an infinite domain is the artificial reflections that are generated at the finite boundaries of the computational grid. These artificial reflections are undesirable because they propagate throughout the computational grid, causing errors in the computed response. The arrival of the artificial reflections can be delayed by placing the grid boundaries in a quiescent region that is far from the region of interest. However, this approach is not economical because the computational region becomes quite large.

The general objective of this effort is to develop a transmitting or energy absorbing boundary for calculations of transient, nonlinear response in an infinite domain. A transmitting or energy absorbing boundary attempts to eliminate the artificial wave reflections from the finite boundaries of the computational grid, allowing the computational domain to be centered on the region of interest.

A number of nonreflecting boundaries have been proposed in the literature. One particular method, called the Incremental Superposition Boundary (ISB), appears to be very efficient and computationally robust for transient calculations. The ISB method (Cundall, et al.) is based on superposition of the solutions for a fixed boundary and for a free boundary. Simple acoustic theory shows that the reflected waves from a fixed and a free boundary are equal in amplitude but opposite in sign; superposition of these two solutions will cancel the reflected waves, leaving the incident pulse.

The specific objective of the present study is to evaluate the ISB method as a transmitting or energy absorbing boundary for transient calculations. Preliminary one-dimensional computational tests showed that the ISB method did not eliminate a reflected wave completely; the amplitude of the reflected wave after cancellation was on the order of 5-12% of

the amplitude of the incident wave. Detailed analyses of the reflection and cancellation process were performed to determine the cause of the errors.

One potential cause of the error in the cancellation process is the finite displacement of points in the computational algorithms. That is, the different displacements of a compression wave and an expansion wave will shift the pulses, causing an error in the cancellation process. A simple perturbation analysis shows that, for small strain elastic response, the effect of finite displacement is negligible compared to the observed cancellation error.

An analytic model was then used to identify the cause of the error in the cancellation process of the ISB method. This model, which is based on a unit step pulse propagating through a one-dimensional computational grid, shows that the cancellation is perfect when the pulse first arrives at the fixed and the free boundaries; but at the next and any subsequent computational cycles, the cancellation has a substantial error if the velocity at the free boundary is not reset properly.

The analytic model also shows that the appropriate velocity at the free boundary has to be modified when the computational time step is less than the maximum stable time step. First- and second-order corrections to the appropriate velocity boundary conditions have been developed for time steps less than the maximum stable time step. Extension of the first- and second-order corrections to two-dimensional problems has not yet been developed.

The theory and the computer implementation for the basic ISB method is discussed in Sections 2.1 and 2.2, respectively. The ISB was incorporated in the Lagrangian, explicit-in-time, finite-difference code STEALTH (Hofmann, 1981), and tested by performing calculations with a cosine pressure pulse propagating through a one-dimensional grid. These calculations will be presented in Section 2.3. The effect of the finite displacement of grid points on the cancellation errors is discussed in Section 2.4.

Section 3 presents the analytic model for identifying the cause of the cancellation error and the derivation of the first- and second-order corrections for the ISB method. The first- and second-order corrections for the modified ISB method are then verified by performing one-dimensional test calculations with STEALTH. These test calculations are also presented in Section 3.

Section 4 is the summary and conclusions from this research.

2.0 DESCRIPTION OF THE ISB METHOD

2.1 THEORY OF THE ISB METHOD

The concept for the Incremental Superposition Boundary (ISB) method is based on a non-reflecting boundary that was developed by Smith (1974) for wave propagation problems. Smith's method calculates the dynamic response of a system in an infinite domain by superimposing the complete solutions for a fixed (Dirichlet) boundary problem and a free (Neumann) boundary problem. The reflected waves from a fixed and a free boundary are equal in amplitude but opposite in sign, so superposition will cancel the reflected waves, leaving the incident wave.

This cancellation can be illustrated for one-dimensional acoustic waves. The displacement, U, of the incident wave in an infinite domain may be expressed as:

$$U = A\, e^{\frac{i\omega}{c}(x - ct)} \tag{2-1}$$

where A is the amplitude of the wave, ω is the frequency, c is the sound speed, x is the position, and t is the time. The displacements for the waves reflected from a fixed and a free boundary are given by :

$$U_{r_{fixed}} = -A\, e^{\frac{i\omega}{c}(-x - ct)} \quad \text{and} \tag{2-2}$$

$$U_{r_{free}} = A\, e^{\frac{i\omega}{c}(-x - ct)}, \quad \text{respectively} \tag{2-3}$$

The total displacements for a fixed and a free boundary problem are then given by superposition as:

$$U_{fixed} = A\, e^{\frac{i\omega}{c}(x - ct)} - A\, e^{\frac{i\omega}{c}(-x - ct)} \tag{2-4}$$

$$U_{free} = A\, e^{\frac{i\omega}{c}(x - ct)} + A\, e^{\frac{i\omega}{c}(-x - ct)} \tag{2-5}$$

The average of Equations (2-4) and (2-5) is then the incident wave, Equation (2-1). Similar arguments also apply to stresses and velocities (in a linear medium). Therefore, the solution for an infinite domain can be obtained by superimposing and averaging the solutions for a fixed and a free boundary problem.

The disadvantage of Smith's method is economics: a number of complete solutions must be computed for various combinations of boundary conditions and wave reflections, and is frequently simpler to just enlarge the computational domain. The ISB method avoids the calculation of complete multiple solutions through an incremental approach. This incremental approach superimposes the fixed and free boundary solutions in two small buffer regions near the boundary, eliminating the reflections from the boundaries as they occur. The dual calculations are only required for the small buffer regions with the ISB method.

2.2 COMPUTER IMPLEMENTATION OF THE ISB METHOD

Figure 2-1 presents a schematic diagram for the structure of the buffer regions and the main grid for the ISB method. Two overlapping buffer regions, A and B, each of three or four zones, are connected independently to the main calculation grid. Region A has a fixed boundary, and region B has a free boundary. For simplicity, a one-dimensional grid is presented in the diagram; the ISB method can be applied to two-dimensional problems.

A wave that propagates from the main grid enters the two buffer regions simultaneously at point p. This wave will then reflect off the fixed and free boundaries of regions A and B. These reflected waves are eliminated by replacing the existing variables in regions A and B with the average values of variables in the two buffer regions. (Each variable of a zone in region A and of the corresponding zone in region B are summed and divided by two. The variables at the nodes connected to the main grid are not averaged.)

This averaging procedure does not have to be performed every cycle because of the stability criterion for explicit-in-time calculations. The ISB method is designed for transient nonlinear problems. These nonlinear problems are usually computed with an explicit-in-time numerical integration scheme. The stability criterion for an explicit calculation requires that the time step be smaller than the time for a wave to travel one zone width. The averaging procedure is then performed once every three or four cycles because the reflected waves cannot propagate into the main grid (or to point p) in less than five cycles.

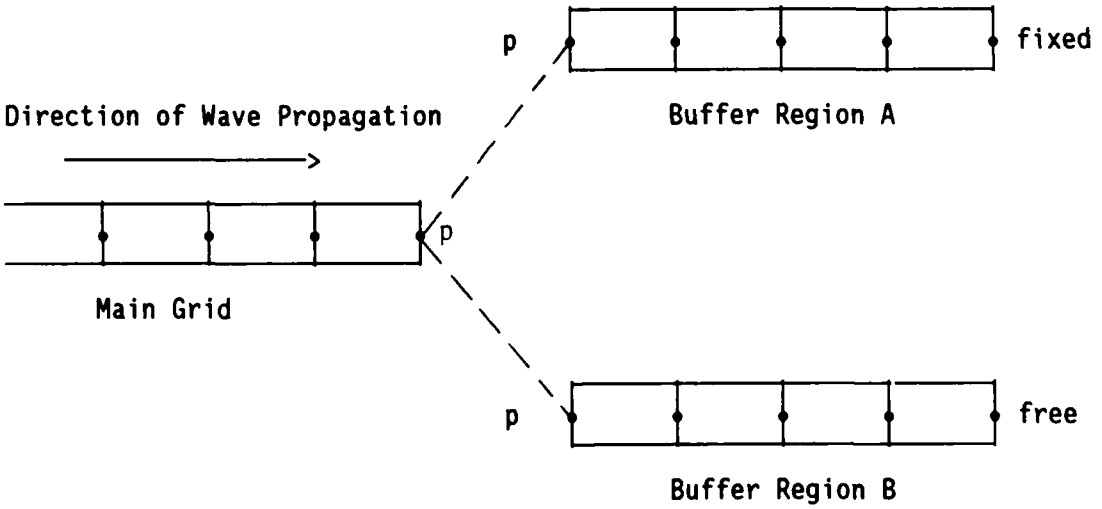

Figure 2-1 A Schematic Diagram of the Buffer Region and the Main Grid for the Incremental Superposition Boundary.

2.3 ONE-DIMENSIONAL COMPUTATIONAL TEST PROBLEM FOR THE ISB METHOD

The ISB model has been incorporated in the Lagrangian, explicit-in-time, finite-difference code, STEALTH (Hofmann, 1984). One-dimensional calculations with a cosine pressure pulse that propagates through the grid are performed to verify the ISB method. The lengths of the main grid and the buffer regions for these test calculations are 42 cm and 4 cm, respectively. All zones are one cm in length, so the main grid contains 42 zones and each buffer region contains 4 zones.

Linear elastic material properties are assumed for the test calculations. The equation of state can be expressed as:

$$P = P_0 + K \left(\frac{\rho}{\rho_0} - 1\right)$$

where P = pressure (Mbar),
P_0 = initial pressure (MBar).
K = bulk modulus (MBar),
ρ_0 = reference density (gm/cc), and
ρ = density (gm/cc).

The initial pressure, the bulk modulus, and the reference density are zero, 0.0022 Mbar, and 1.0 gm/cc, respectively. The pressure boundary condition that generates the cosine pressure pulse is given by:

$$P = 5 \times 10^{-6} (1 - \cos \omega t),$$

where t = time in μs,
and $\omega = 0.02 \pi \ \mu s^{-1}$.

Three calculations were performed with time step safety factors of 0.95, 0.67 and 0.50. The time step safety factor is the ratio of the computational time step to the maximum stable time step. Typical values of the time step safety factor range from 0.5 to 0.95; the default value for STEALTH is 0.67.

Figures 2-2(a), 2-3(a), and 2-4(a) present pressure time-history plots at a point in the main grid, 3 cm from the inside edge of the buffer region. The large pulse, centered at 300 μsec, is the incident wave; the smaller waves after 360 μsec are the reflected waves from the ISB. (If the ISB were perfect, only the large pulse would appear in these figures.) The three figures are for time step safety factors of 0.95, 0.67, and 0.50, respectively.

Figures 2-2(b), 2-3(b), and 2-4(b) present pressure-distance plots at 500 μsec, when the incident wave has propagated beyond the ISB, and the reflected wave is centered in the main grid. (If the ISB were perfect, no reflected pulse would appear in the figures.) These plots show the amplitude and time dependence of the reflected waves on the same scale as the first set of figures. Figures 2-5 through 2-7 present the same pressure-distance plots in an enlarged scale.

These results show that the original ISB method does not eliminate the reflected wave completely; the amplitude of the reflected wave after cancellation is on the order of 5-12% of the amplitude of the incident wave, and is a function of the magnitude of the time step (or the time step safety factor).

2.4 EFFECT OF FINITE DISPLACEMENT OF THE COMPUTATIONAL GRID POINTS

Computational results from the previous section show that the ISB method has a substantial error in the cancellation process. One potential cause of this cancellation error is the finite displacement of grid points in the computational algorithms. That is, the different displacements of a compression wave and an expansion wave will shift the pulses, causing an error in the cancellation process.

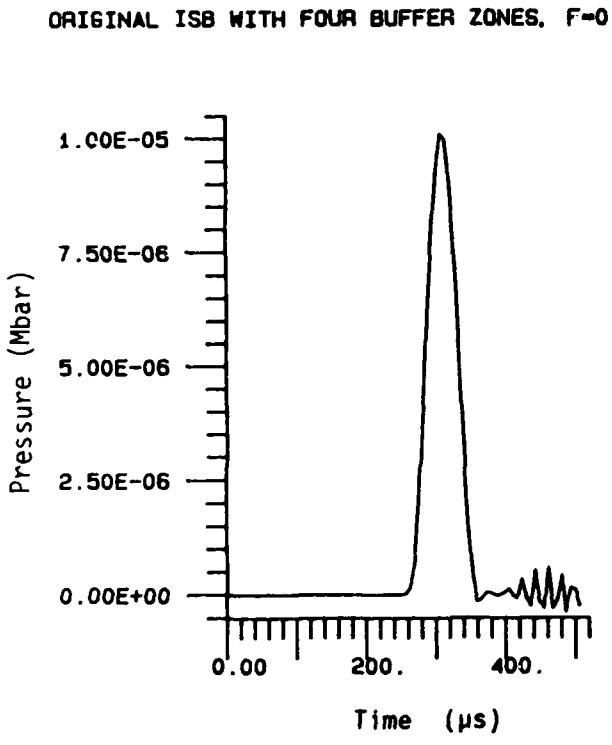

(a) Pressure-time history at x = 39 cm

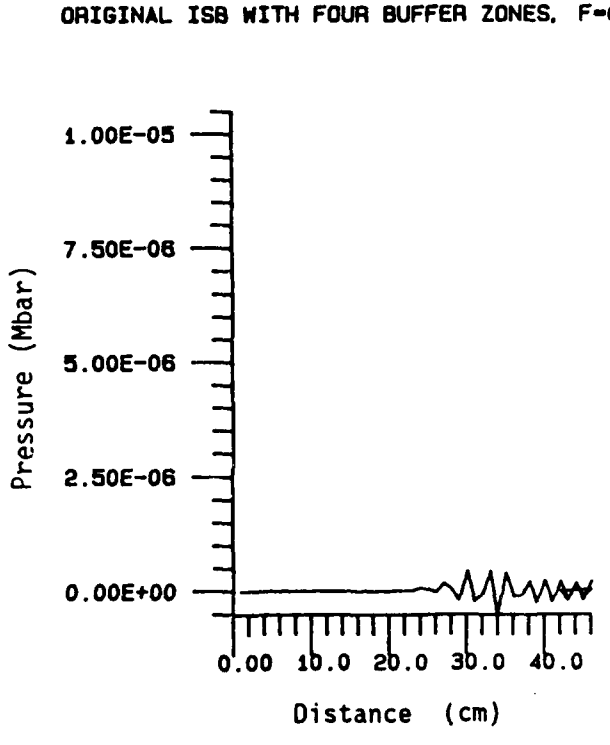

(b) Pressure-distance plot at 500 μs for the reflected wave

Figure 2-2 Pressure Plots for the Original ISB with Four Buffer Zones. Time Step Safety Factor is 0.95.

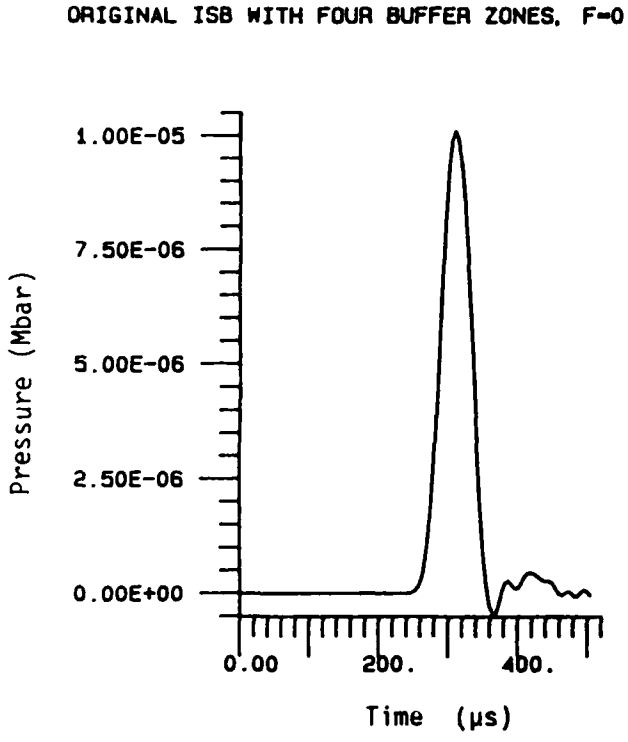

(a) Pressure-time history at x = 39 cm

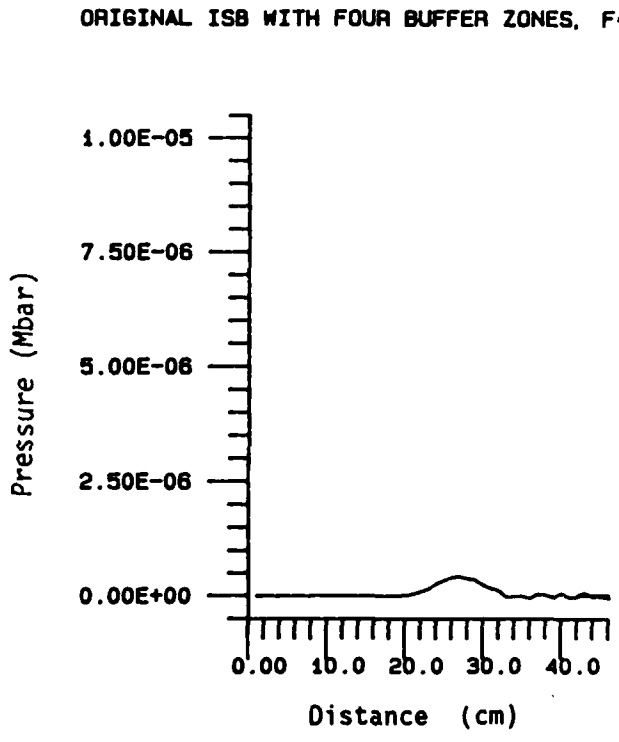

(b) Pressure-distance plot at 500 μs for the reflected wave

Figure 2-3 Pressure Plots for the Original ISB with Four Buffer Zones. Time Step Safety Factor is 0.67.

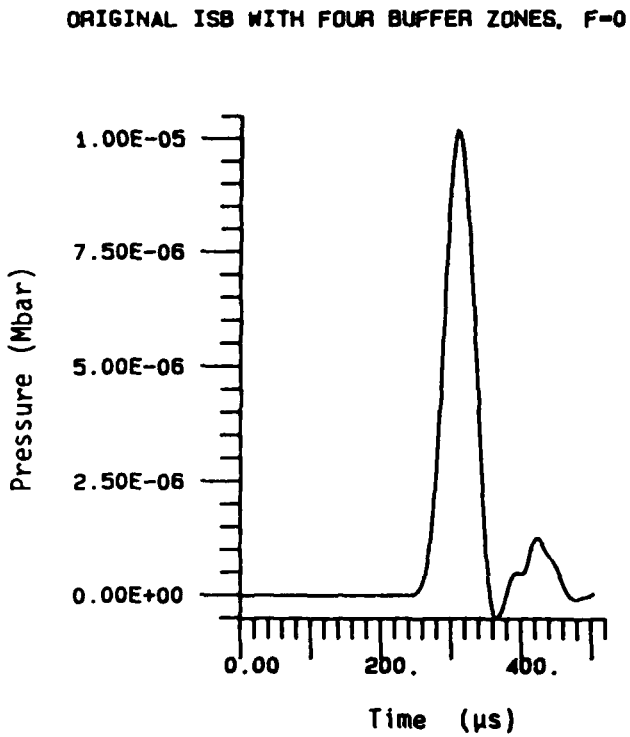

(a) Pressure-time history at x = 39 cm

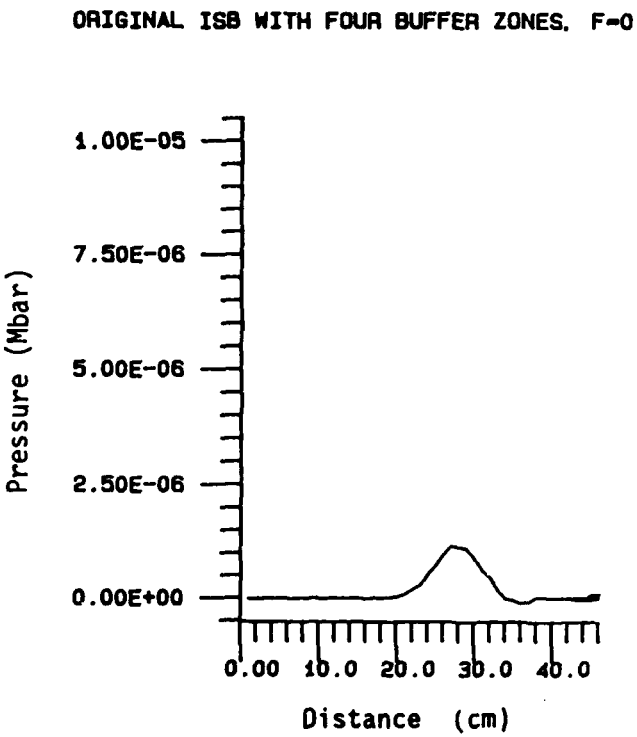

(b) Pressure-distance plot at 500 μs for the reflected wave

Figure 2-4 Pressure Plots for the Original ISB with Four Buffer Zones. Time Step safety Factor is 0.50.

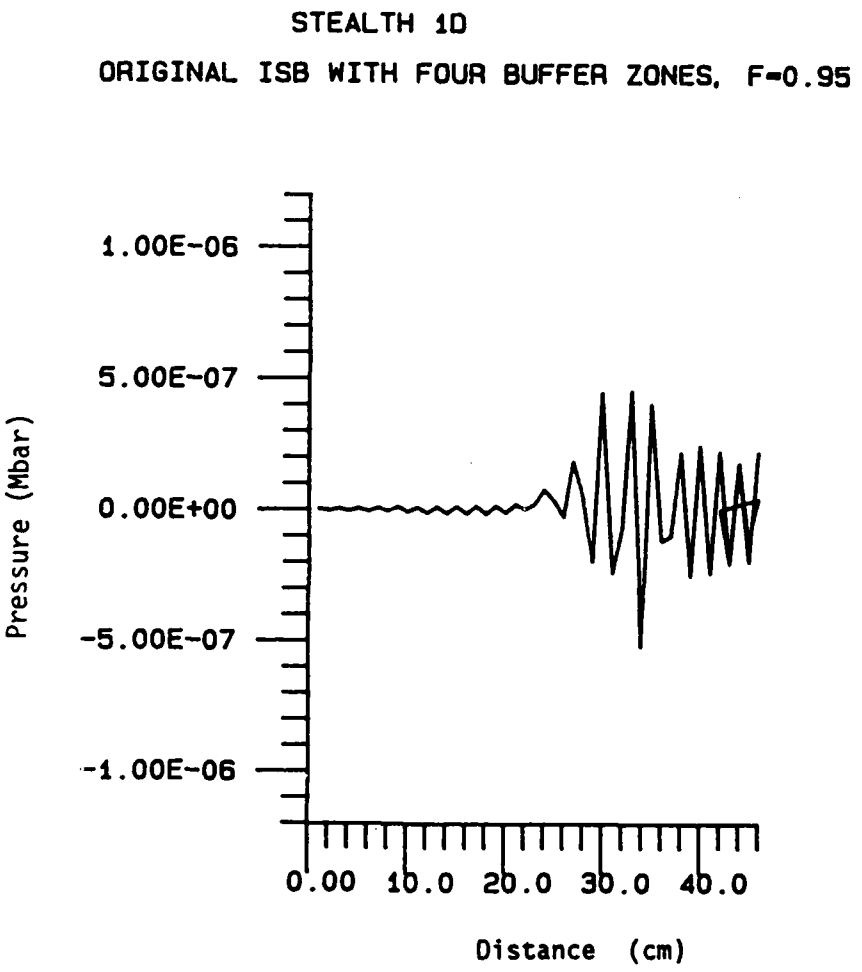

Figure 2-5 Pressure-distance Plot at 500 μs for the Reflected Wave for the Original ISB. Time Step Safety Factor is 0.95.

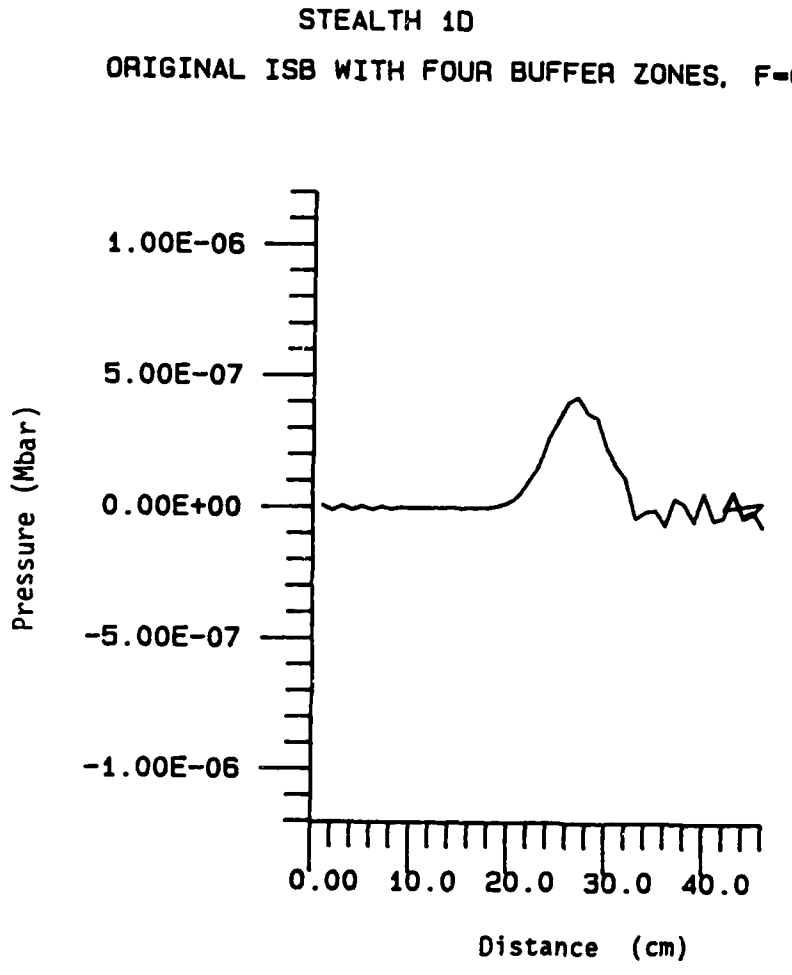

Figure 2-6 Pressure-distance Plot at 500 μs for the Reflected Wave for the Original ISB. Time Step Safety Factor is 0.67.

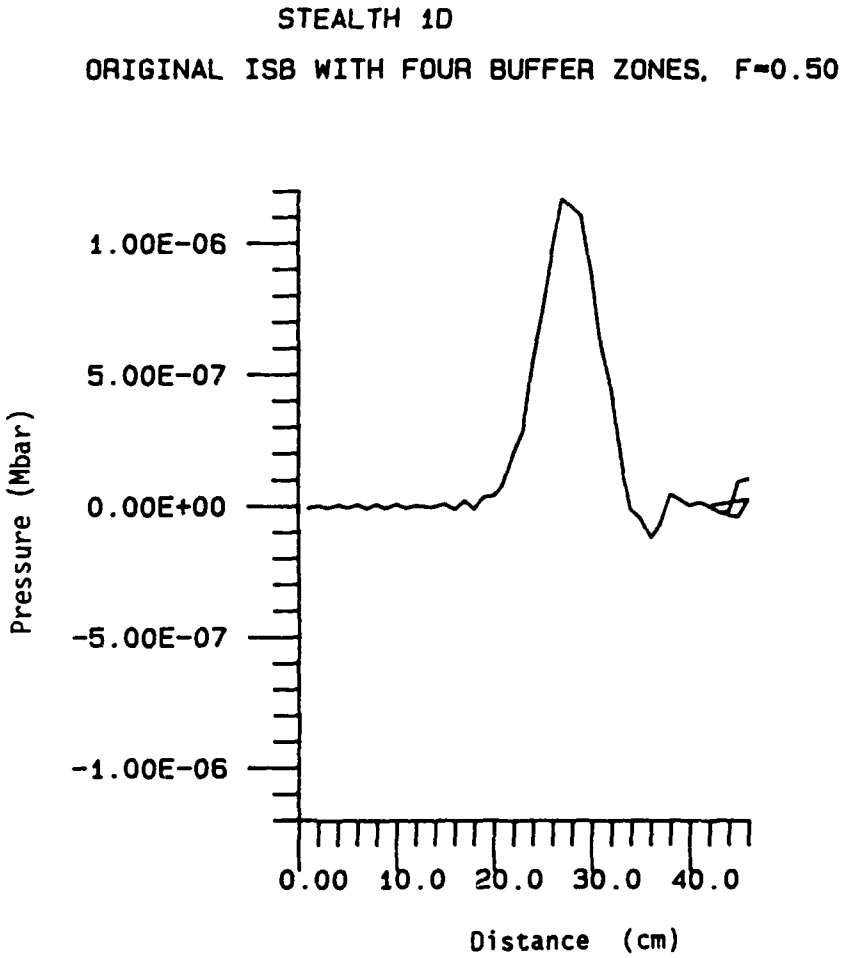

Figure 2-7 Pressure-distance Plot at 500 μs for the Reflected Wave for the Original ISB. Time Step Safety Factor is 0.50.

A simple perturbation analysis can estimate the magnitude of the error due to the finite displacement of the computational grid. The velocities of the reflected wave from the fixed and the free boundary can be expressed as:

$$V_{r_{fixed}} = - A\, e^{\frac{i\omega}{c}(-x - ct)} \tag{2-6}$$

$$V_{r_{free}} = A\, e^{\frac{i\omega}{c}(-x - ct)} \tag{2-7}$$

where V_r = velocity of the reflected wave (cm/μs),
A = amplitutde of the incident (or the reflected) wave (cm/μs),
x = position (cm)
ω = frequency (MHz),
c = sound speed (cm/μs), and
t = time (μs).

The error, E, of the velocity of the reflected wave due to the finite displacement of the grid points can be obtained by perturbing Equation (2-7) with respect to ω and x. Then the error can be expressed as:

$$E = \left| \frac{\partial V_{r_{free}}}{\partial x} dx + \frac{\partial V_{r_{free}}}{\partial \omega} dw \right| \tag{2-8}$$

Substituting Equation (2-7) into Equation (2-8), the error, E, becomes

$$E = \left| \frac{iA}{c}\, e^{\frac{i\omega}{c}(-x - ct)} \quad (w dx + (x + ct) dw \right|$$

$$\leq \left| A\, (\omega dx + (x + ct) d\omega) / c \right|. \tag{2-9}$$

The maximum displacement, dx, of a grid point for the test problem discussed in Section 2-3 is found by integration of the velocity for the period of the incident wave. Acoustic theory (Currie, 1974) shows that the velocity, v(t), of an acoustic wave is given by :

$$v(t) = P_b(t)\, c / K, \tag{2-10}$$

where $P_b(t)$ is the pressure at the boundary, c is the sound speed, and K is the bulk modulus. The maximum displacement is then:

$$dx = \int_0^T \frac{c\ 5\times10^{-6}}{K} (1 - \cos \omega t)\, dt = 0.00337 \text{ cm.}$$

where T = period of the wave = 100 μs,
c = $\sqrt{(K/\rho)}$ = 0.1483 cm/μs,
ρ = density = 1 gm/cc, and
K = bulk modulus = 0.022 Mbar.

The perturbation in ω, $d\omega$, can be estimated as:

$$d\omega = \omega - \frac{2\pi}{T + dx/c} = 1.43\times10^{-5}\ \mu s^{-1},$$

where ω = frequency = 0.02π MHz.

Substituting these values of dx and $d\omega$ into Equation (2-9), the normalized error, $|E/A|$, for the test problem in Section 2-3 is found to be 0.00286. The same argument can be applied for pressure and displacement.

The result from this perturbation analysis shows that the cancellation error from the finite displacement is approximately 0.3%, well below the observed error and below the level of numerical noise in the calculation. (The value of 0.3% is valid for the specific pulse and material properties that are used in the numerical calculations. The magnitude of the error will vary with pulse amplitude, pulse shape, and bulk modulus.)

3.0 ANALYSIS OF THE ISB METHOD

3.1 IDENTIFICATION OF THE CAUSE OF THE CANCELLATION ERROR

The cause of the cancellation error in the ISB method has been identified by a simple analytic model with a step pulse propagating through a computational grid. The pressure pulse is allowed to propagate into two separate buffer grids with a fixed and a free boundary, and the solutions of these two grids are averaged at the end of each computational cycle. The initial pressure is p_0, and the step pulse is generated by a constant pressure, p_1, at the upstream boundary. This model assumes one-dimensional grids with two equal zones of length L and a linear elastic medium.

The equation of state for a linear elastic material can be expressed as:

$$p = p_0 + K \left(\frac{\rho}{\rho_0} - 1\right) \tag{3-1}$$

where p = pressure,
p_0 = initial pressure,
K = bulk modulus,
ρ_0 = reference density and,
ρ = density.

For a small strain problem, the equations of state and motion at cycle n can be expressed in finite-difference form as:

$$p_i^n = \frac{K}{L} \left(D_{i-1}^n - D_i^n\right) , \tag{3-2}$$

$$u_i^{n+1/2} = u_i^{n-1/2} + \frac{dt}{\rho L} \left(p_i^{n-1} - p_{i+1}^{n-1}\right), \tag{3-3}$$

$$D_i^n = D_i^{n-1} + u_i^{n+1/2}\, dt, \tag{3-4}$$

where p_i^n = pressure at the center of the i^{th} zone,

$u_i^{n+1/2}$ = velocity of the i^{th} grid point,

D_i^n = displacement of the i^{th} grid point

and dt = time step

The velocity and displacement of the free boundary before averaging are

$$u_k^{n+1/2} = u_k^{n-1} + \frac{2\,dt}{\rho\,L}\,p_i^{n-1} \qquad (3\text{-}5)$$

and $$D_i^n = D_i^{n-1} + u_i^{n+1/2}\,dt \quad \text{,respectively.} \qquad (3\text{-}6)$$

The following diagrams show the cycle-by-cycle cancellation process of the ISB method as the pressure pulse propagates through the grid. In these diagrams, D and u denote displacement and velocity of the grid point, respectively, p denotes pressure at the center of the zone, and U denotes the velocity behind the step pulse, $(p_1-p_0)/(\rho c)$. The values of D, u, and p for each grid or zone are computed according to Equations (3-2) through (3-6). The maximum stable time step (dt = L/c, c=sound speed) is assumed for each cycle.

The cycle-by-cycle response of the grids is as follows:

- At cycle 0, the grids are quiescent, except for the step change in pressure and velocity on the left boundary.

- At cycle 1, the pulse has propagated one zone width into the grids. The response in both grids is identical because the pulses have not arrived at the right boundaries. Averaging is not shown because the states are unchanged.

- At cycle 2, the pulse has propagated two zone widths into the grids. The response is still identical and averaging is not shown.

- At cycle 3, the pulses first reflect off the fixed and free boundaries. Averaging produces perfect cancellation, in the sense that only the incident wave remains after averaging.

- At cycle 4, after the second reflection from the fixed and free boundaries, the averaging produces pressures that are different than the pressure, p_1, in the incident pulse.

Initially at cycle 0:

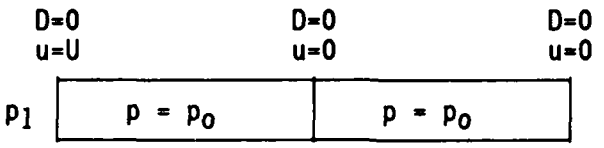

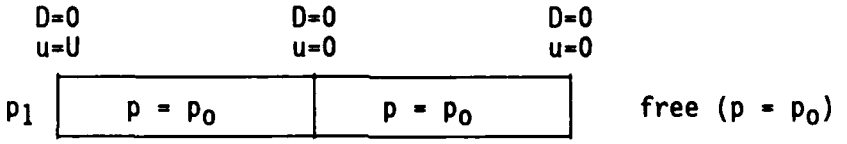

At cycle 1

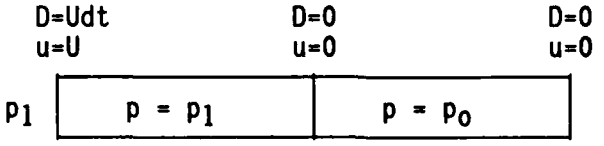

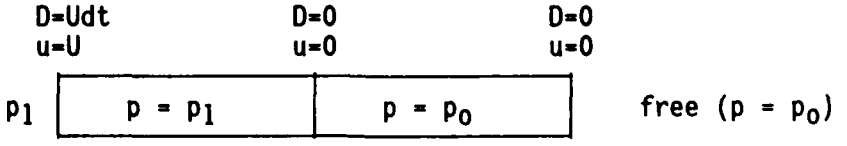

At cycle 2

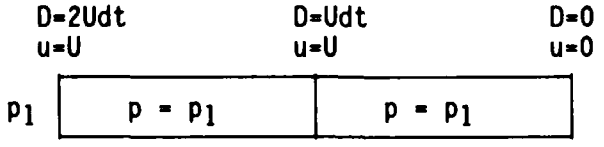

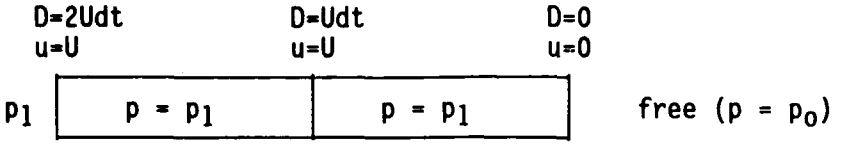

At cycle 3 before averaging

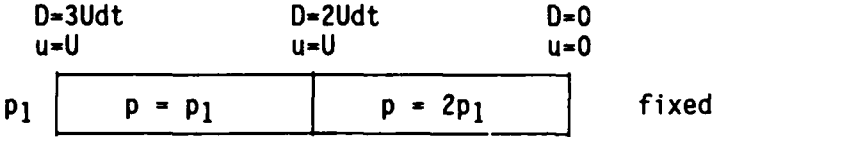

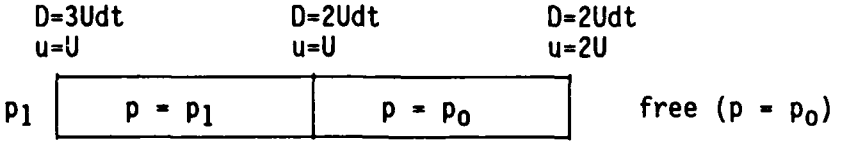

At cycle 3 after averaging

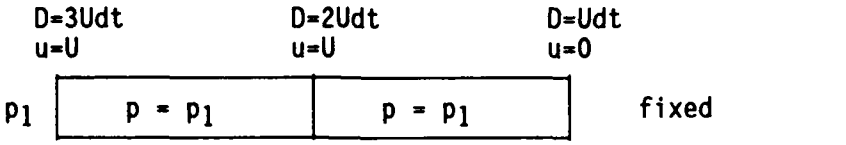

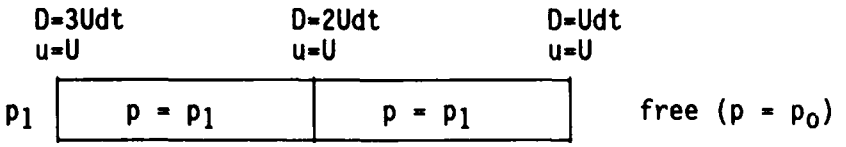

(note that the cancellation is perfect)

At cycle 4 before averaging

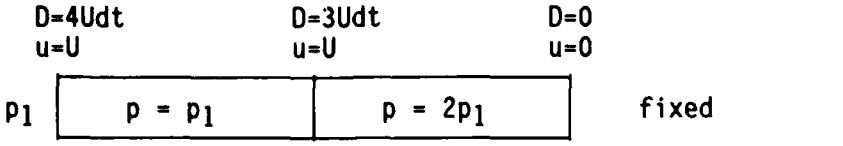

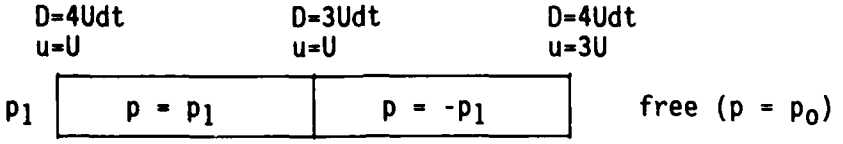

At cycle 4 after averaging

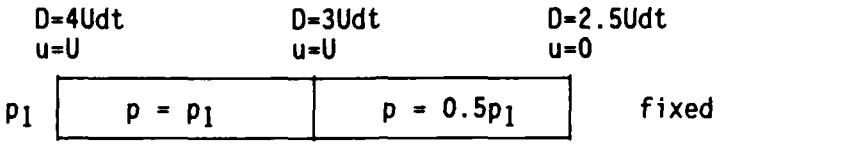

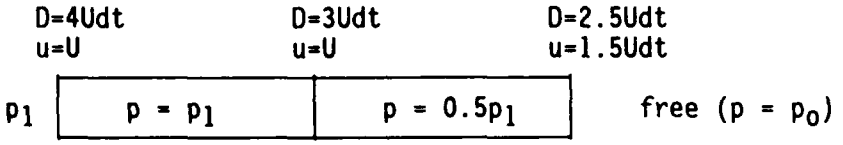

The above analysis shows perfect cancellation when the wave first arrives at the fixed and free boundaries at cycle 3. However, at the next cycle, the cancellation error is substantial; the magnitude of the reflected wave is 50% of the amplitude of the incident wave. This error will persist if more zones are used in this analysis. The reflected wave will oscillate about zero stress, and the magnitude of the reflected wave can be up to 50% of the magnitude of the incident wave. This error will also occur with more complex pulse shapes because complex pulses can be generated from superposition of simple step pulses (for small strain problems with linear elastic materials).

An analysis of the simple analytic model shows that the cancellation error occurs because the velocity of the free boundary is not reset properly after the averaging process.

3.2 VELOCITY CORRECTION FOR MAXIMUM STABLE TIME STEP

The analytic model discussed in Section 3.1 shows that the ISB method can completely cancel the reflected wave at the fourth cycle if the velocity at the free boundary is reset to zero. The analytic model also implies that only one boundary zone is required for cancelling the reflected waves although the original ISB method averages three to four zones adjacent to the boundaries.

A one-dimensional computational test was performed with STEALTH to verify the ISB method with the velocity at the free boundary reset to zero at the beginning of each cycle. The calculation is performed at the maximum stable time step. The length of the computational grid is 42 cm, excluding the one-zone buffer region that is 1 cm wide. The parameters for the linear elastic material and for the pressure boundary are identical to the parameters for the previous calculations.

Figure 3-1 presents the pressure-time history plot for a point near the transmitting boundary (39 cm from the pressure boundary or 3 cm from the inner boundary of the buffer zone) and the pressure-distance plot for the reflected wave. Figure 3-2 presents the pressure-distance plot of the reflected wave in an enlarged scale at 500 μs, when the reflected wave is at the middle of the main grid. These results show that the amplitude of the wave reflected from the transmitting boundary is 0.075 bar, which is 0.75% of the amplitude of the incident wave. The amplitude of the reflected wave is insignificant because the noise level of a wave reflected from a free boundary is on the order of 0.4% of the incident wave.

3.3 FIRST-ORDER CORRECTION FOR LESS THAN MAXIMUM STABLE TIME STEP

Computational tests showed that the cancellation error of the ISB method is still substantial when the time step is less than the maximum stable time step, even though the velocity at the free boundary is reset

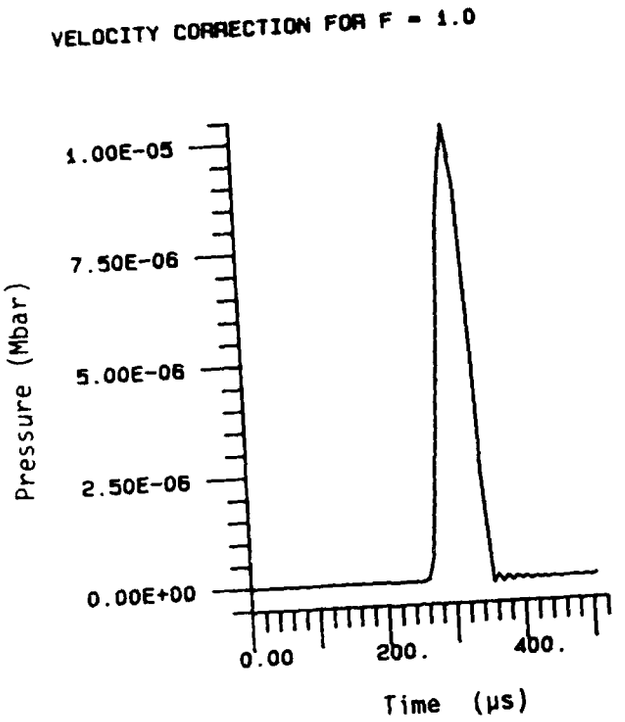

(a) Pressure-time history at x = 39 cm

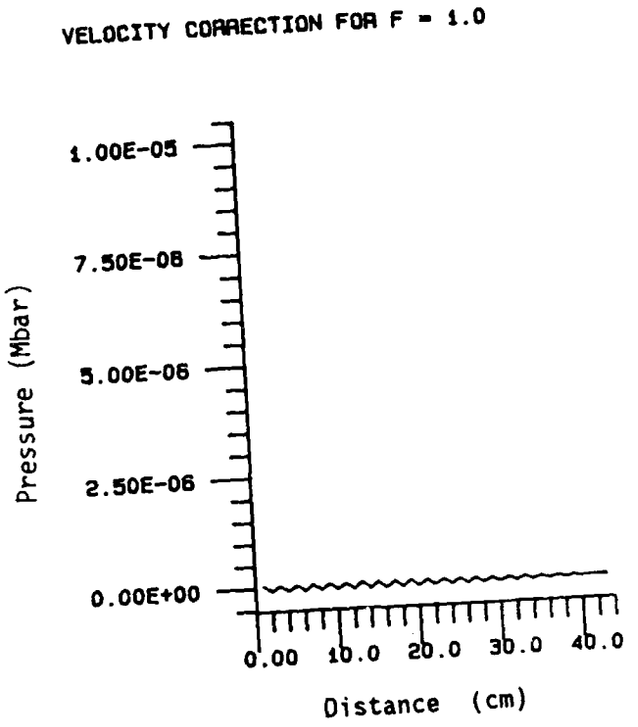

(b) Pressure-distance plot at 500 μs for the reflected wave

Figure 3-1 Pressure Plots for the ISB with the Velocity of the Free Boundary reset to Zero at the Beginning ot Each Cycle. Time Step safety Factor is one.

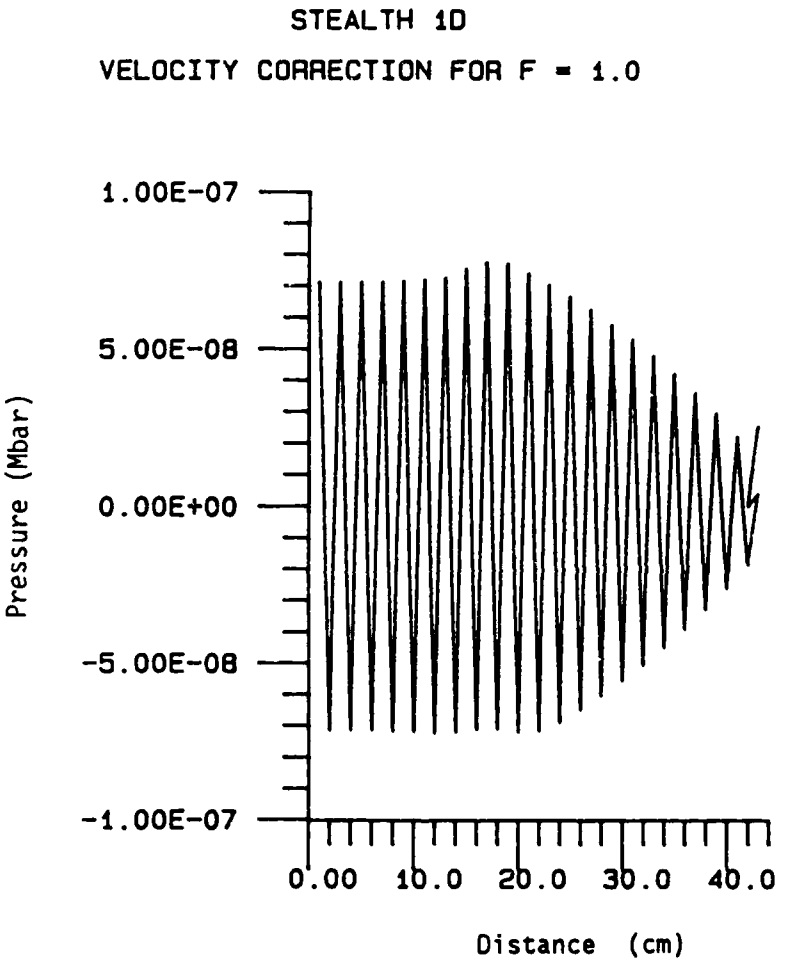

Figure 3-2 Pressure-distance Plot at 500 μs for the Reflected Wave for the ISB with the Velocity of the Free Boundary Reset to Zero at the Beginning of Each Cycle. Time Step Safety Factr is one.

to zero at the beginning of each cycle. Therefore, the velocity correction for the free boundary has to be modified for a time step less than the maximum stable time step.

A first-order correction for the velocity at the free boundary has been developed for a time step less than the maximum stable time step. Identical expressions for this first-order correction can be derived from two different approaches. The first approach is based on a comparison of the numerical solutions for a computational grid with ISB and for a computational grid with a boundary at infinity. The second approach is based on an approximation to the stress at the boundary of the computational grid.

First Approach

The first-order correction for the velocity at the free boundary can be derived by considering a linear pressure (or velocity) ramp propagating through a computational grid with ISB and through a computational grid with the boundary at infinity. The computational grid assumes equal zones. The initial n cycles are computed at the maximum stable (and constant) time step until the leading edge of the ramp arrives at the ISB; the subsequent cycles are computed at time steps less than the maximum stable time step. Then the velocities (u) and stresses (σ) at cycle n for the infinite grid can be expressed as:

$$u_i^{n+1/2} = (n - i)\,\frac{d\sigma}{\rho L}\,dt_{max} \qquad (1 \le i \le n) \qquad (3\text{-}7)$$

and $$\sigma_i^n = (n + 1 - i)\,d\sigma, \qquad (1 \le i \le n) \qquad (3\text{-}8)$$

where $d\sigma$ = stress increment per cycle at the boundary,
L = length of a zone,
and dt_{max} = maximum stable time step.

At cycle n + 1, the velocity of the k^{th} grid point of the infinite grid is

$$u_k^{n+1+1/2} = u_k^{n+1/2} + \frac{d\sigma}{\rho L}\,f\,dt_{max} \qquad (3\text{-}9)$$

where $f = dt/dt_{max}$ = the time step, safety factor, and dt is the time step for cycle n + 1.

The velocities and stresses of the ISB grid are also given by Equations (3-7) and (3-8), except that i is less than or equal to k, where k is the total number of grid points in the main grid and buffer. If the velocity at the free boundary is reset to $U^{n+1/2}$ at the beginning of the cycle n+1, the velocity at the free boundary after averaging is given by:

$$u_{k\,free}^{n+1+1/2} = \frac{1}{2}\left[U_f^{n+1/2} + \frac{d\sigma}{0.5\,\rho\,L}\,(n+1-k)\,f\,dt_{max}\right]. \quad (3\text{-}10)$$

Note that the grid point at the free boundary has only half a zone width between the stress at the center of the zone and the stress on the free boundary. Since the velocity at the free boundary after cancellation must be identical to the velocity of the k^{th} grid, $U_f^{n+1/2}$ can be evaluated by equating Equations (2-9) and (2-10). Then the first order correction for the velocity of the free boundary, $U_f^{n+1/2}$, can be expressed as:

$$U_f^{n+1/2} = 2\,u_k^{n+1/2} - 2\,\frac{d\sigma}{\rho\,L}\,(n-k)\,f\,dt_{max}$$

$$= 2(1-f)\,u_k^{n+1/2}. \quad (3\text{-}11)$$

If the initial n cycles are not computed at the maximum stable time step and the velocity at the free boundary is reset at the beginning of the cycle according to Equation (3-11), the velocity at the free boundary at cycle n can be expressed as:

$$u_{k\,free}^{n+1/2} = \frac{1}{2}\left[2(1-f)\,u_{k\,free}^{n-1/2} + \frac{2}{\rho\,L}\,\sigma_k^{n-1}\,f\,dt_{max}\right]$$

$$= u^{n-1/2}_{k_{free}} + \frac{1}{\rho L} f\, dt_{max} \left[\sigma^{n-1}_k - \sum_{j=1}^{n-1} f(1-f)^{j-1} \sigma^{n-1-j}_k \right] \quad (3\text{-}12)$$

Second Approach

The second approach to derive the first-order correction for the velocity at the free boundary is based on an estimate of the stress in a phantom zone at the boundary. This phantom zone has an identical zone length as the boundary zone. The new stress of the phantom zone is estimated by a linear interpolation of the stresses in the phantom boundary zone and in the buffer zone.

A schematic diagram for this linear interpolation is presented in Figure 3-3. For a linear elastic problem, the wave propagates a length of cdt (cdt = fL) per computational cycle, where c is the sound speed, dt is the computational time step, f is the time step safety factor, and L is the zone length. If constant time steps are assumed for every cycle, the stress at the phantom zone, σ^n_b, and the velocity at the free boundary, $u^{n+1/2}_{k_{free}}$, can be expressed as:

$$\sigma^n_b = f\, \sigma^{n-1}_k + (1-f)\, \sigma^{n-1}_b$$

$$= f \sum_{j=1}^{n} (1-f)^{j-1} \sigma^{n-j}_k \quad \text{and} \quad (3\text{-}13)$$

$$u^{n+1/2}_{k_{free}} = u^{n-1/2}_{k_{free}} + \frac{1}{\rho L} f\, dt_{max} (\sigma^{n-1}_k - \sigma^{n-1}_b)$$

$$= u^{n-1/2}_{k_{free}} + \frac{1}{\rho L} f\, dt_{max} \left[\sigma^{n-1}_k - \sum_{j=1}^{n-1} f(1-f)^{j-1} \sigma^{n-1-j}_k \right]. \quad (3\text{-}14)$$

Note that the boundary zone is treated as an interior zone which has a full zone mass and width rather than half width values. This is equivalent to adding the stress given by Equation (3-13) to the free boundary and doubling the velocity at the free boundary at the beginning of each cycle.

Since Equation (3-14) is identical to Equation (3-12), the velocity corrections at the free boundary given by Equation (3-11) are identical for both approaches. Note that for the maximum stable time step (f=1) the velocity correction given by Equation (3-11) is equivalent to resetting

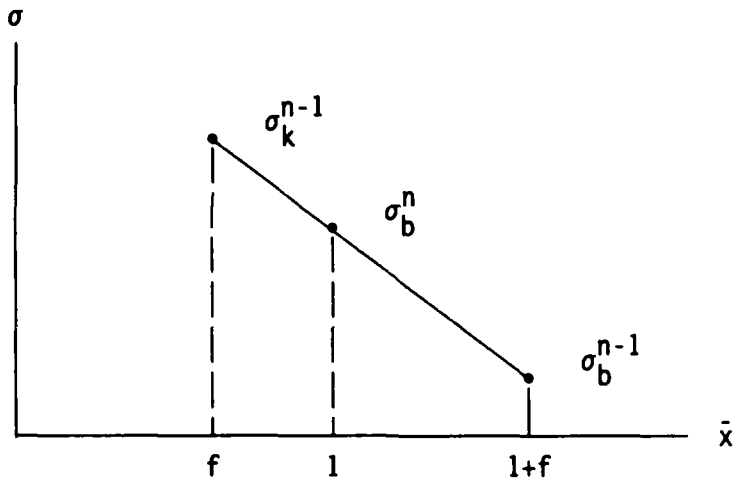

Note $\bar{x} = \dfrac{x - x_k}{L}$,

σ = stress,

x = position,

x_k = position of the center of the boundary zone,

L = one zone length, and

f = time step safety factor.

Figure 3-3 A Schematic Diagram for Determining the Stress of the Phantom Zone by a Linear Interpolation.

boundary velocity to zero. This is consistent with the velocity correction discussed in Section 3.2 for maximum stable time step. Similarly, the displacements and stresses can be shown to be identical for both approaches.

A one-dimensional test calculation was performed with STEALTH. This calculation is identical to that discussed in Section 3.2 except that the time step was less than the maximum stable time step and the velocity at the free boundary was reset at the beginning of each cycle according to Equation (3-11).

Figures 3-4 through 3-6 present the pressure-time history plots of the incident wave and the pressure-distance plots of the reflected wave for a time-step safety factor of 0.95, 0.67, and 0.50, respectively. Figures 3-7 through 3-9 present, in an enlarged scale, the pressure-distance plots of the reflected wave for the same time-step safety factors. The pressure-distance plot is taken at 500 μs, when the wave front of the reflected wave is at the middle of the main grid. These results show that the amplitudes of the reflected waves are 0.6, 1.8, and 2.9% of the amplitude of the incident wave for a safety factor of 0.95, 0.67, and 0.50, respectively. Note that these errors are much lower than the errors for the original ISB method. The cancellation errors for the original ISB method are on the order of 5 to 12% of the amplitude of the incident wave.

The residual cancellation errors for the ISB method with velocity correction appear to be caused by a second-order effect, related to the rate of change of pressure. This effect probably occurs because a time step less than the maximum stable time step causes nonlinear numerical diffusion, while the velocity correction is based on a linear interpolation for the stress at the phantom boundary zone.

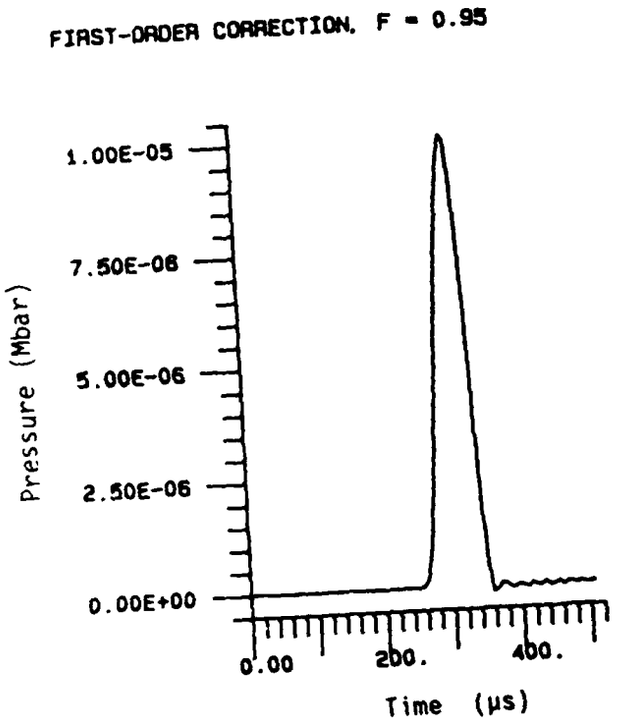

(a) Pressure-time history at x = 39 cm

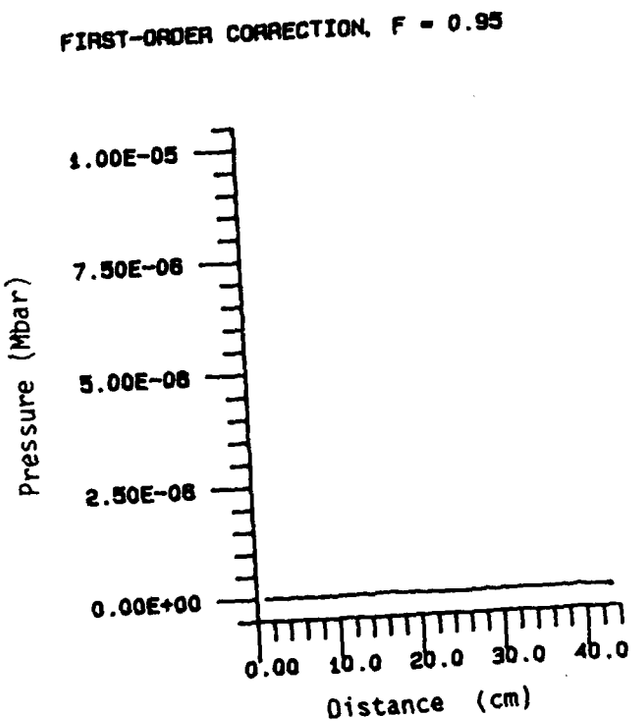

(b) Pressure-distance plot at 500 μs for the reflected wave

Figure 3-4 Pressure Plots for the ISB with the First-order Correction. Time Step safety Factor is 0.95.

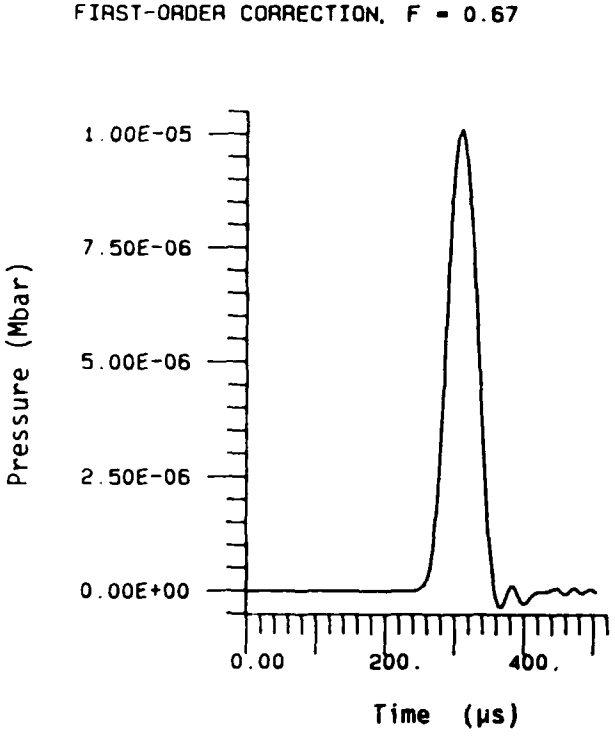

(a) Pressure-time history at x = 39 cm

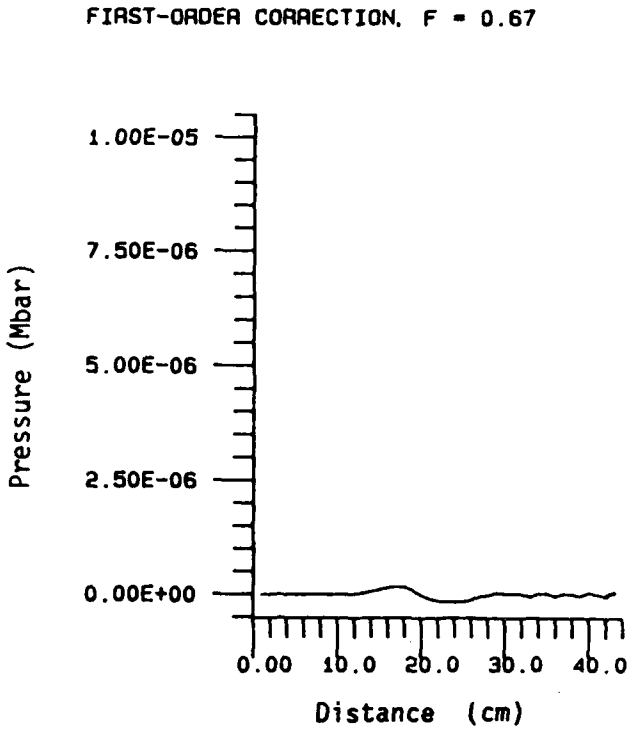

(b) Pressure-distance plot at 500 μs for the reflected wave

Figure 3-5 Pressure Plots for the ISB with the First-order Correction. Time Step safety Factor is 0.67.

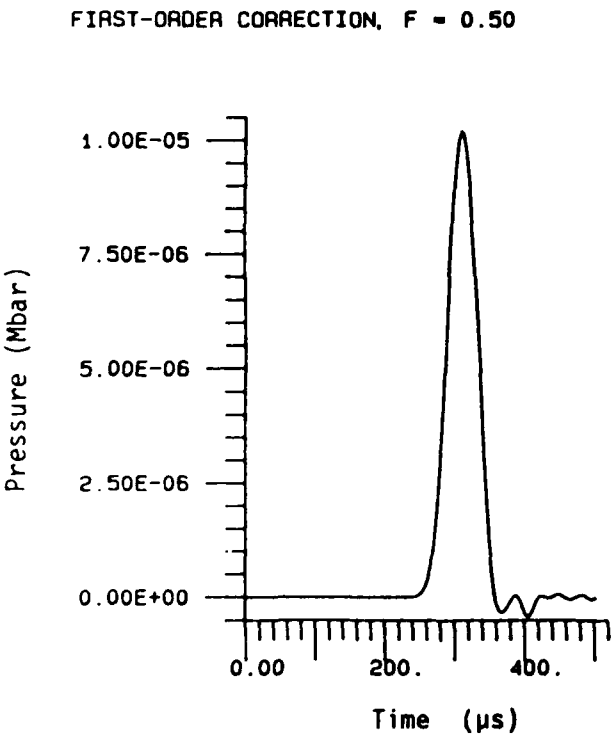

(a) Pressure-time history at x = 39 cm

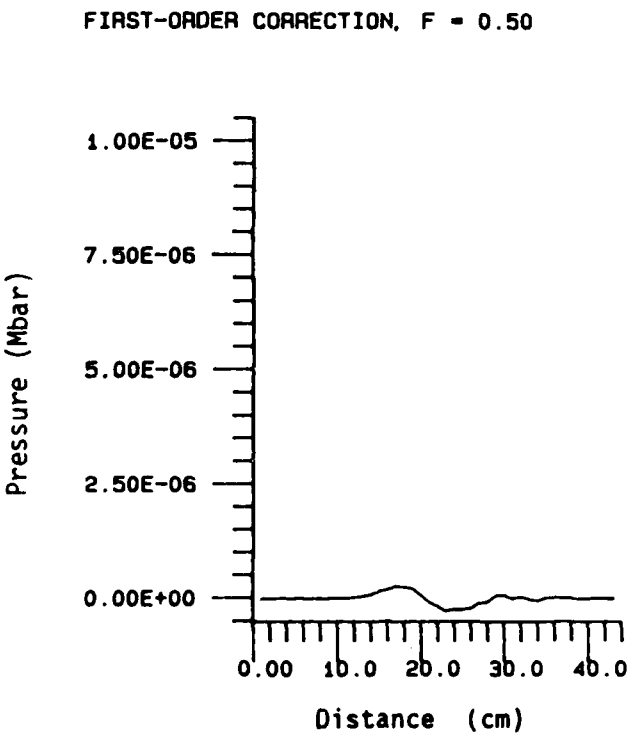

(b) Pressure-distance plot at 500 μs for the reflected wave

Figure 3-6 Pressure Plots for the ISB with the First-order Correction. Time Step safety Factor is 0.50.

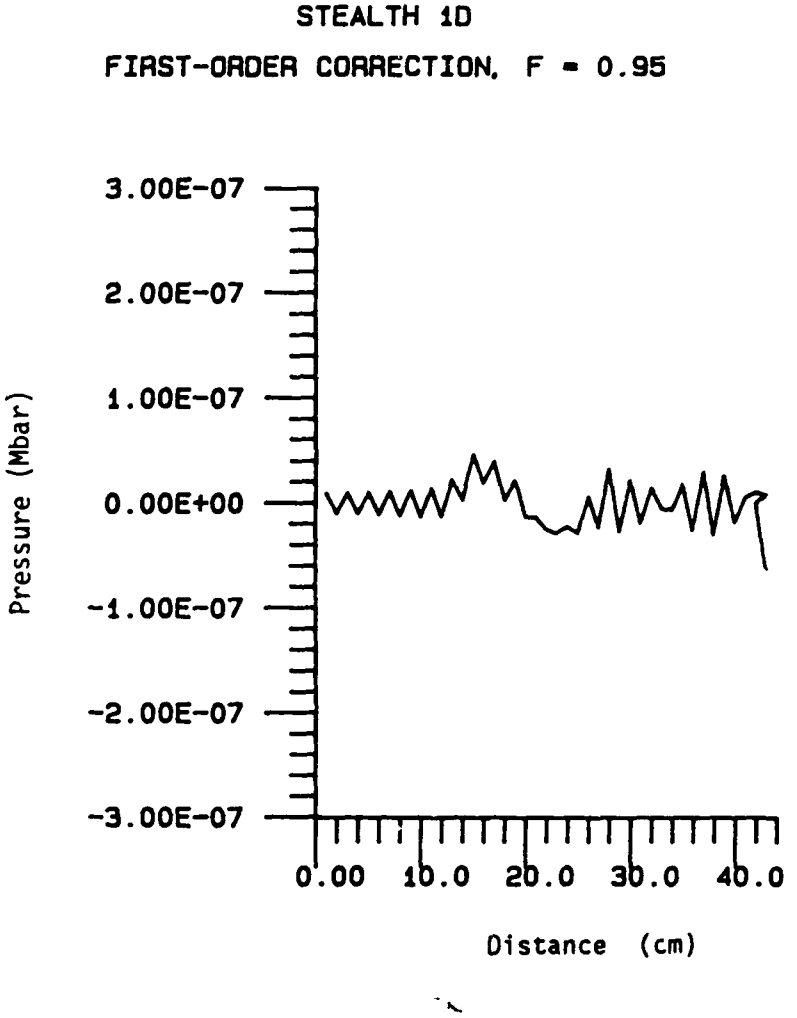

Figure 3-7 Pressure-distance Plot at 500 μs for the Reflected Wave for the ISB with the First-order Correction. Time Step Safety Factor is 0.95.

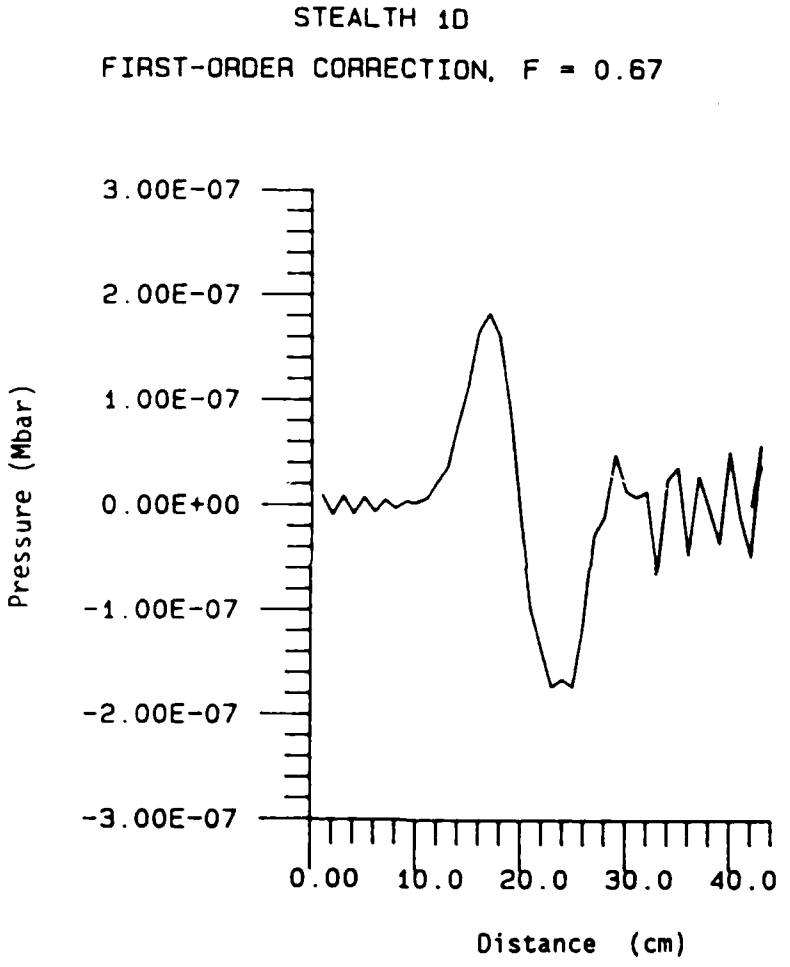

Figure 3-8 Pressure-distance Plot at 500 μs for the Reflected Wave for the ISB with the First-order Correction. Time Step Safety Factor is 0.67.

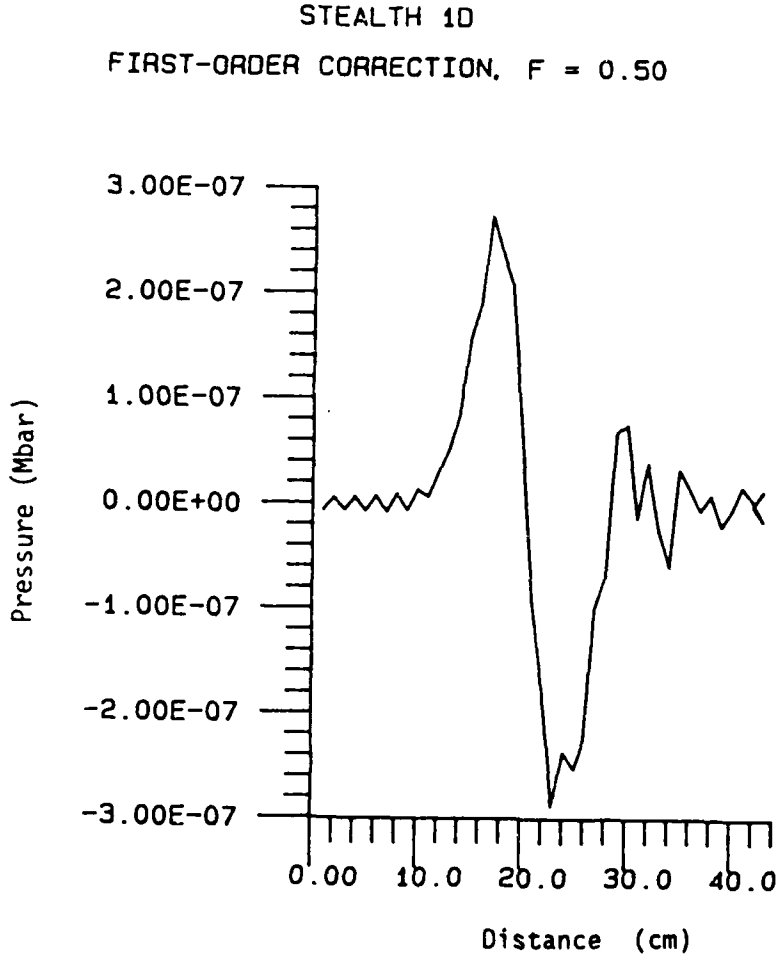

Figure 3-9 Pressure-distance Plot at 500 μs for the Reflected Wave for the ISB with the First-order Correction. Time Step Safety Factor is 0.50.

3.4 SECOND-ORDER CORRECTION FOR LESS THAN MAXIMUM STABLE TIME STEP

Even though the cancellation errors of the ISB method for a time step less than the maximum stable time step can be reduced by a first-order correction for the velocity at the free boundary, the level of the errors is still on the order of 0.6% to 2.9% of the amplitude of the incident wave. A second-order correction for the ISB method has been developed for reducing the cancellation errors to the order of the computational noise level, which is about 0.4% of the amplitude of the incident wave. The derivation of this second-order correction is based on the extension of the second approach discussed in Section 3.3; the stress at the phantom boundary zone is estimated by a quadratic fit rather than a linear interpolation.

Figure 3-10 presents a schematic diagram for estimating the phantom boundary zone by a quadratic fit. Assuming the stress at the phantom boundary zone satisfies the following quadratic equation:

$$\sigma_b^n = a\,\bar{x}^2 + b\bar{x} + c\ ,$$

where σ_b^n = stress at the boundary phantom zone,

$\bar{x} = (x - x_k) / L$,

L = one zone length,

x = position of the center of the phantom boundary zone,

x_k = position of the center of the zone adjacent to the boundary,

The coefficients a, b, and c are determined by the following conditions:

at $\bar{x} = 0$, $\sigma_b^n = \sigma_k^n$,

at $\bar{x} = f$, $\sigma_b^n = \sigma_k^{n-1}$; and

at $\bar{x} = 2f$, $\sigma_b^n = \sigma_k^{n-2}$;

where σ_k^n is the stress of the boundary zone at cycle n, and f is the time step safety factor.

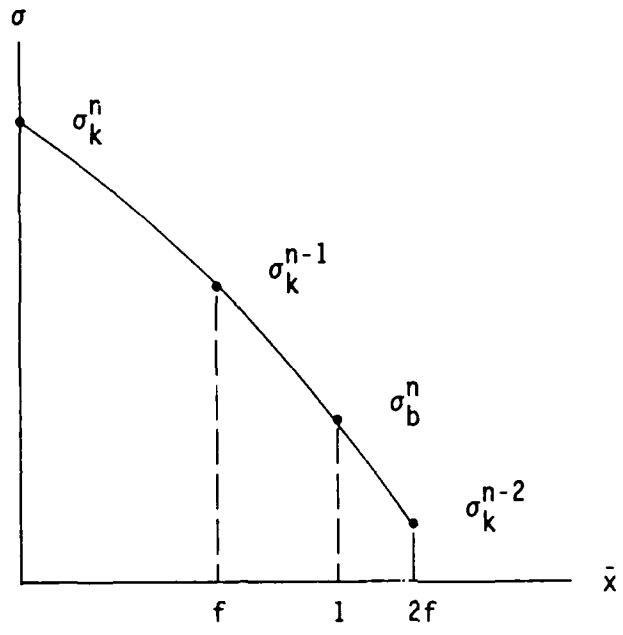

Note $\bar{x} = \dfrac{x - x_k}{L}$,

σ = stress,

x = position,

x_k = position of the center of the boundary zone,

L = one zone length, and

f = time step safety factor.

Figure 3-10 A Schematic Diagram for Determining the Stress of the Phantom Zone by a Quadratic Fit.

The stress in the phantom boundary zone, which is located at $\bar{x} = 1$, is given by:

$$\sigma_b^n = \frac{2f^2 - 3f + 1}{2f^2} \sigma_k^n + \frac{2f - 1}{f^2} \sigma_k^{n-1} + \frac{1 - f}{2f^2} \sigma_k^{n-2} . \quad (3\text{-}15)$$

Again, to calculate the velocity at the boundary, the boundary zone must be treated as an interior zone which has a full zone width and mass. This is equivalent to adding the stress given by Equation (3-15) to the free boundary and doubling the velocity at the free boundary at the beginning of each cycle. Then the velocity at the free boundary after cancellation can be expressed as:

$$u_{k_{free}}^{n+1/2} = u_{k_{free}}^{n-1/2} + \frac{1}{\rho L} f \, dt_{max} (\sigma_k^{n-1} - \sigma_b^{n-1}) \quad (3\text{-}16)$$

For a time-step safety factor of one, Equations (3-12), (3-14), and (3-16) are identical and are equivalent to resetting the velocity of the free boundary to zero at the beginning of each cycle. This is consistent with the velocity correction for the maximum stable time step (Section 3.2).

One-dimensional test calculations identical to those discussed in Section 3.2 were performed with STEALTH, except that the time step was less than the maximum stable time step, the velocity at the free boundary was reset by doubling it at the beginning of each cycle, and the stress given by Equation (3-14) was added to the free boundary.

Figures 3-11 through 3-13 present the pressure-time history plots of the incident wave and the pressure-distance plots of the reflected wave for a time-step safety factor of 0.95, 0.67, and 0.5, respectively. Figures 3-14 through 3-16 present, in an enlarged scale, the pressure-distance plots of the reflected wave for the same time-step safety factors. These pressure-distance plots are taken at 500 μs when the wave front of the reflected wave is at the middle of the main grid. The results of the calculations show that the amplitude of the reflected waves is less than 0.6% of the amplitude of the incident wave for all safety factors. This level of error is insignificant because the computational noise level of a wave reflected from a free boundary is on the order of 0.4% of the incident wave.

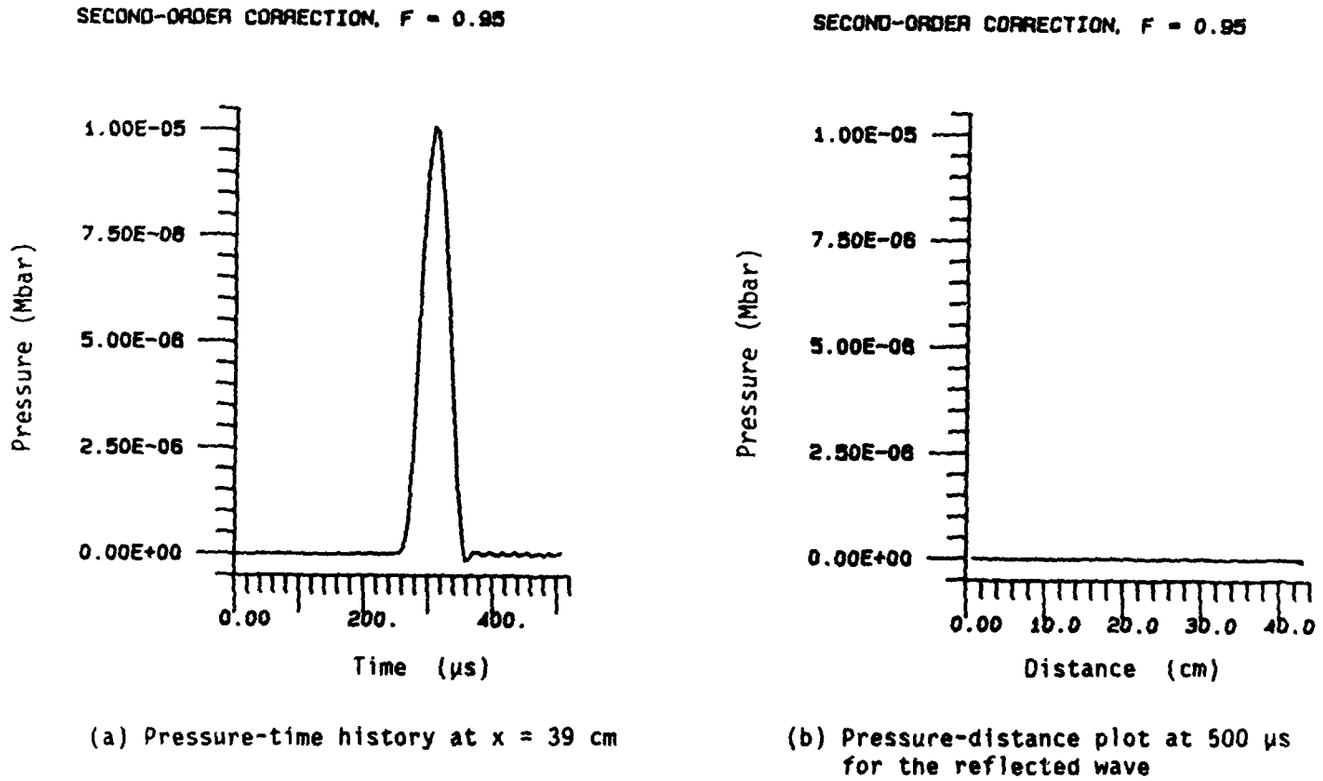

(a) Pressure-time history at x = 39 cm

(b) Pressure-distance plot at 500 μs for the reflected wave

Figure 3-11 Pressure Plots for the ISB with the Second-order Correction. Time Step safety Factor is 0.95.

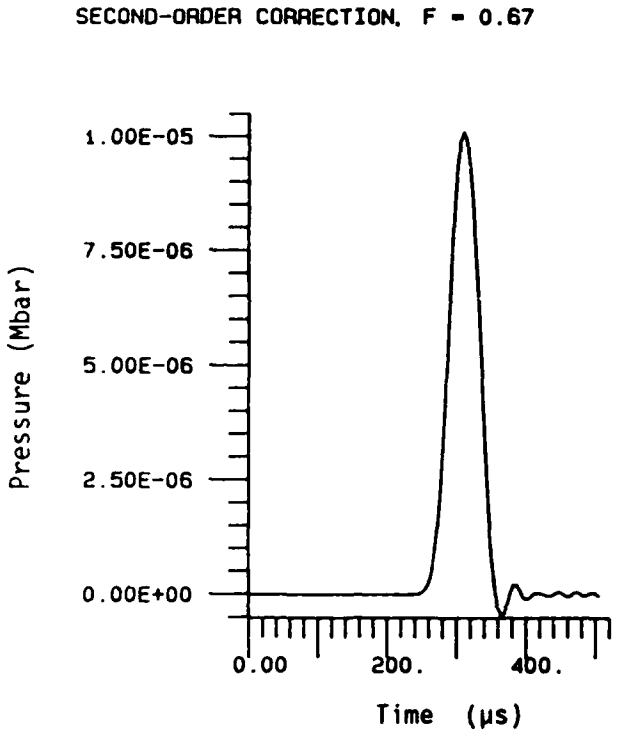

(a) Pressure-time history at x = 39 cm

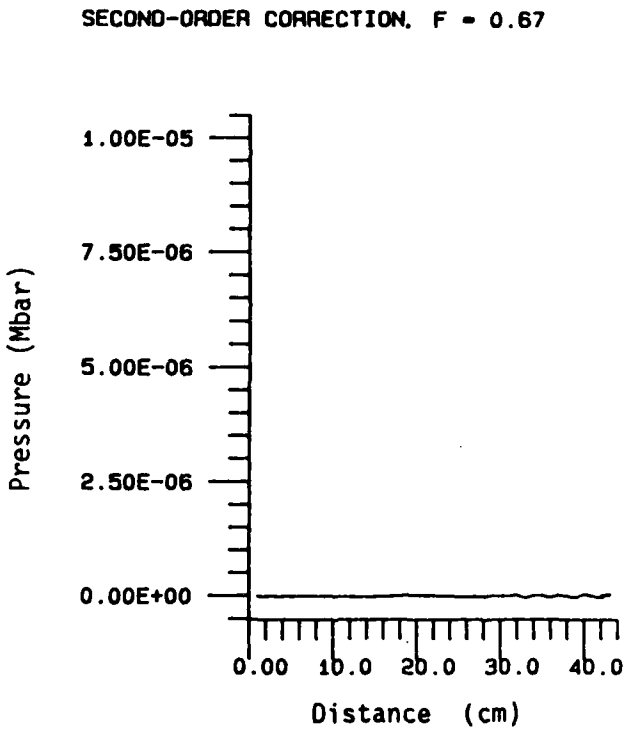

(b) Pressure-distance plot at 500 μs for the reflected wave

Figure 3-12 Pressure Plots for the ISB with the Second-order Correction. Time Step safety Factor is 0.67.

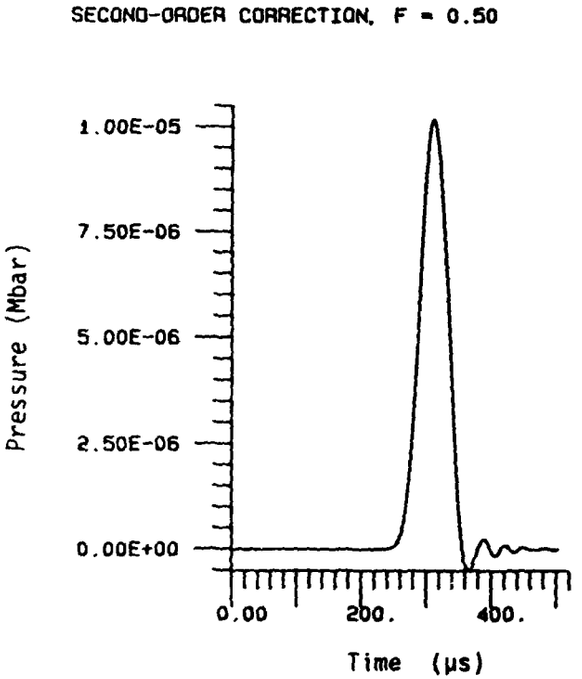

(a) Pressure-time history at x = 39 cm

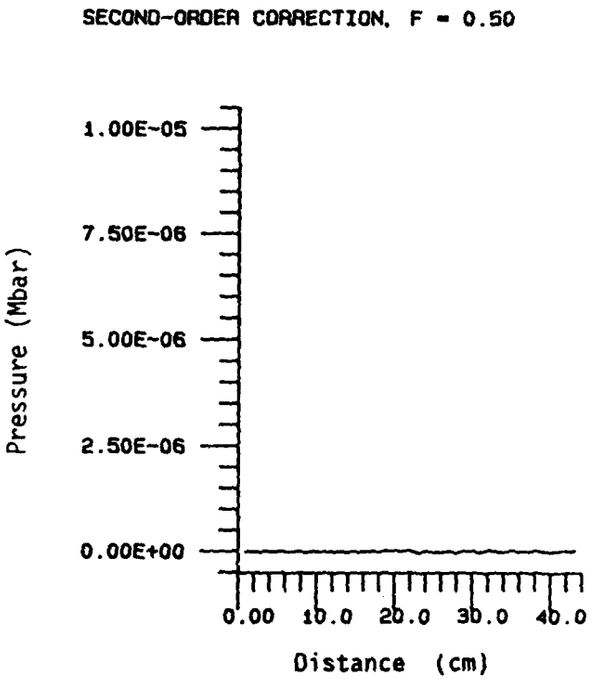

(b) Pressure-distance plot at 500 μs for the reflected wave

Figure 3-13 Pressure Plots for the ISB with the Second-order Correction. Time Step safety Factor is 0.50.

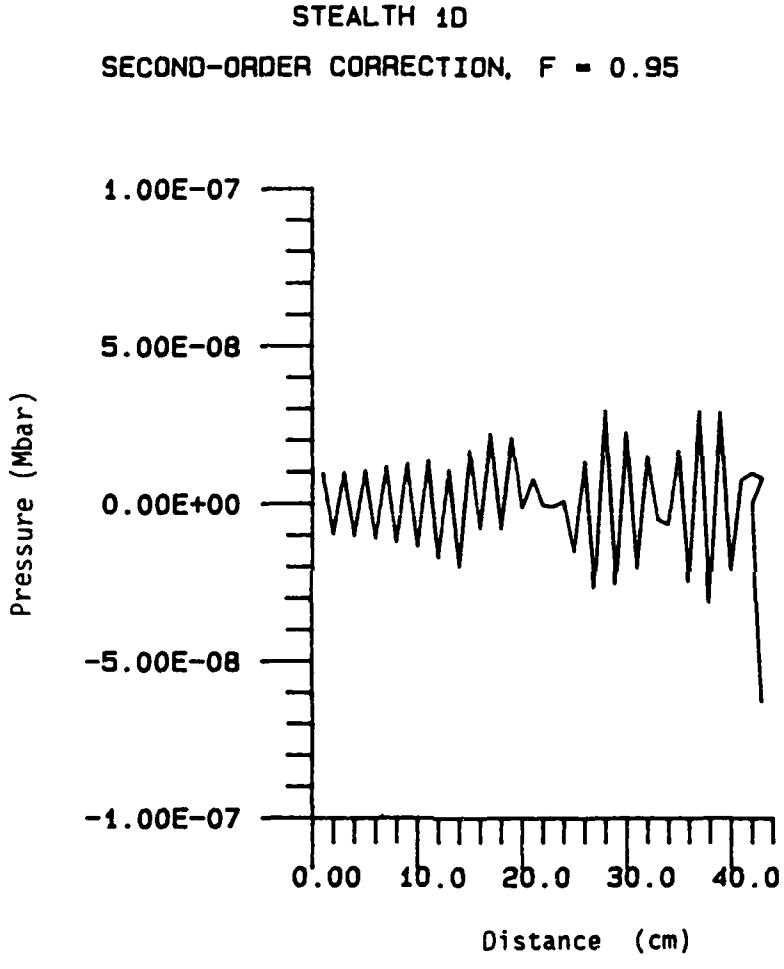

Figure 3-14 Pressure-distance Plot at 500 μs for the Reflected Wave for the ISB with the Second-order Correction. Time Step Safety Factor is 0.95.

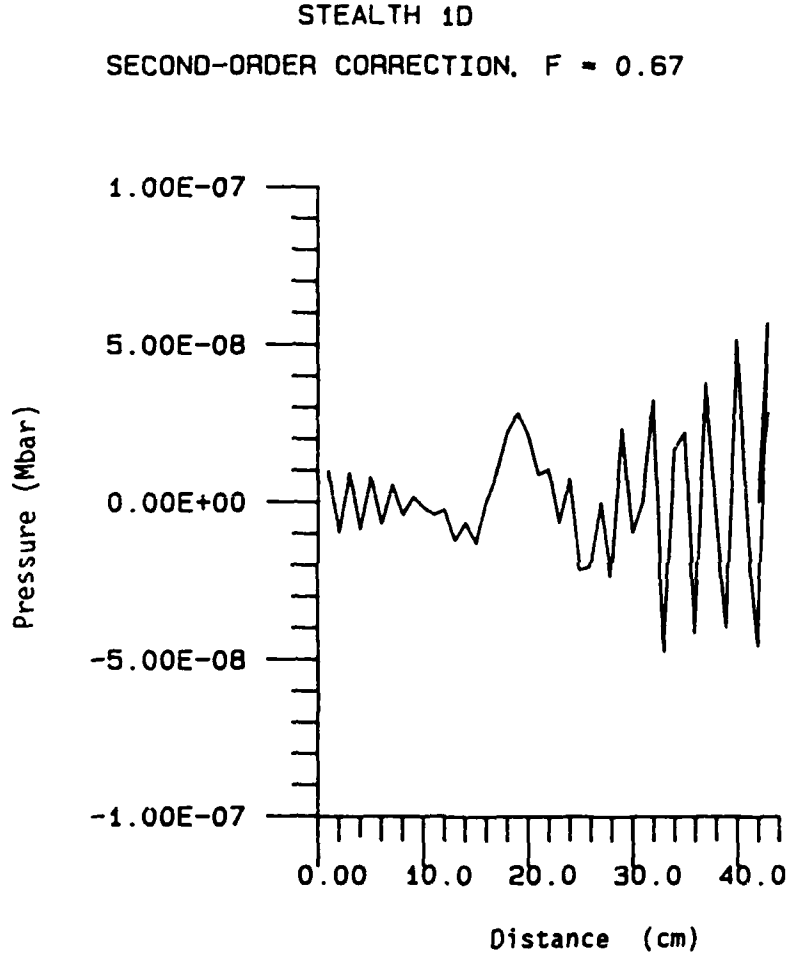

Figure 3-15 Pressure-distance Plot at 500 μs for the Reflected Wave for the ISB with the Second-order Correction. Time Step Safety Factor is 0.67.

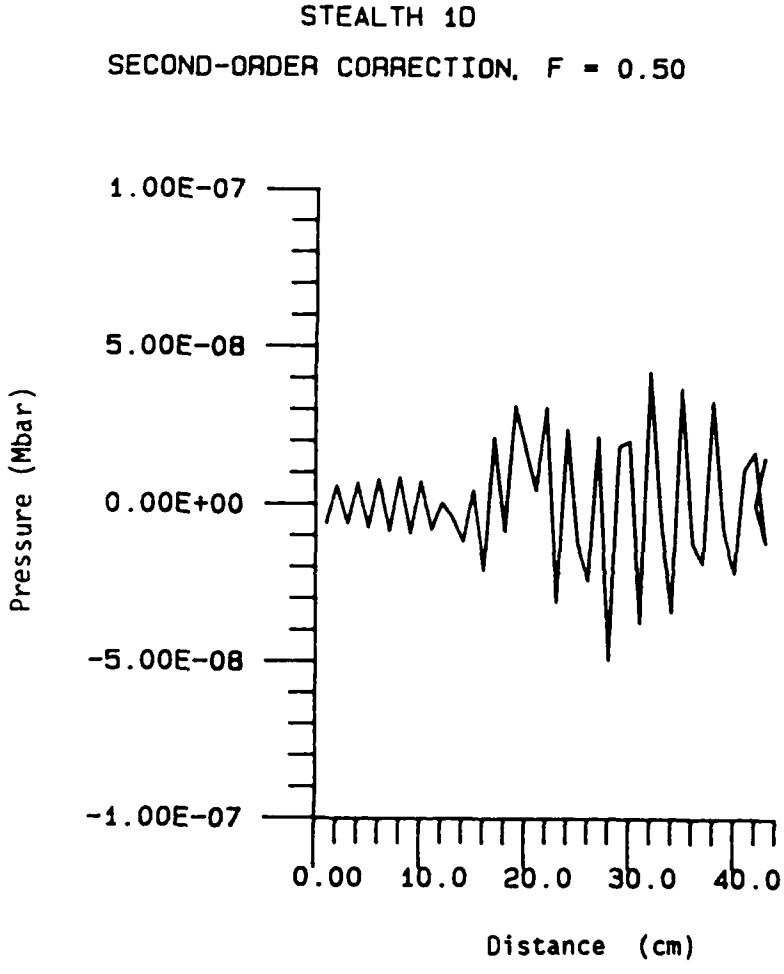

Figure 3-16 Pressure-distance Plot at 500 μs for the Reflected Wave for the ISB with the Second-order Correction. Time Step Safety Factor is 0.50.

4.0 CONCLUSIONS

A transmitting or energy absorbing boundary for one-dimensional calculations of nonlinear system response in an infinite domain has been developed. These transmitting boundaries are based on the incremental superposition boundary developed by Cundall et al. A first- or second-order correction to the ISB greatly reduces the magnitude of the reflected wave for all time step safety factors. In addition, only one zone in the buffer region is required for ISB with the first- or the second-order correction, whereas the original ISB requires a buffer region of three to four zones.

Calculations with a cosine pressure pulse propagating through a one-dimensional grid were performed for the original ISB and for the modified ISB with the first- and second-order corrections. These calculations were performed with a Lagrangian, explicit-in-time, finite-difference code STEALTH. The results of these calculations for the magnitude of the reflected wave are summarized in Table 4-1. These results indicate that the ISB with the first- or second-order corrections is more effective in cancelling the reflected waves than the original ISB. In particular, the second-order correction reduces the level of the cancellation error to the order of the computational noise, which is about 0.4% of the amplitude of the incident wave for a wave reflected from a free boundary.

Although the level of cancellation is good, the presence of the time step safety factor, f, in the corrections is undesirable for multi-dimensional calculations. In two-dimensional calculations, the effective safety factor for shear and dilation waves is different because the sound speed of both waves is different. The presence of the safety factor then implies that a simple velocity correction factor will peroform equally well for the two different wave types. It may be possible to cancel the waves by adjusting the shear stress on the boundary. In addition the reflected waves may also be dispersed by the two-dimensional reflection process. Further analysis is necessary to extend the modified ISB to two-dimensional calculations.

Table 4-1 Comparison of the Magnitude of the Reflected Wave for the Original and Modified ISB

	Ratio of the Magnitude of the Reflected to the Incident Wave		
	Time Step Safety Factors		
	0.95	0.67	0.50
The Original ISB	5%	5%	12%
ISB with First-order Correction	0.6%	1.8%	2.9%
ISB with Second-order Correction	0.6%	0.5%	0.5%

5.0 REFERENCES

Cundall, P.A., R. R. Kunar, P. C. Carpenter, J. Marti. Solution of Infinite Dynamic Problems by Finite Modelling in the Time Domain, Advanced Technology Group, Dames and Moore, London.

Currie, I. G., Fundamental Mechanics of Fluids, McGraw-Hill Inc., pp. 356-371, 1974.

Hofmann, R., 1981; STEALTH - A Lagrange Finite Difference Code for Solids, Structural, and Thermohydraulic Analysis, EPRI NP-2080, Volumes 1A, 1B, 2, and 3, prepared by Science Applications International Corporation for Electric Power Research Institute, Palo Alto, California.

Smith, W. D., "A Nonreflecting Plane Boundary for Wave Propagation Problems", Journal of Computational Physics, Volume 15, pp. 492-503, 1974.IN-FINITE MEDIA

END

DATE

FILMED

5-88

DTIC